

FOCUS ISSUE ON ELECTROCHEMICAL DEPOSITION AS SURFACE CONTROLLED PHENOMENON

Hydrogen Sorption Kinetics on Bare and Platinum-Modified Palladium Nanofilms, Grown by Electrochemical Atomic Layer Deposition (E-ALD)

Kaushik Jagannathan, David M. Benson, David B. Robinson, b, and John L. Stickney, Etickney, and John L. Stickney, and John L. Stickn

^aDepartment of Chemistry, University of Georgia, Athens, Georgia 30602, USA

Nanofilms of Pd were grown using an electrochemical form of atomic layer deposition (E-ALD) on 100 nm evaporated Au films on glass. Multiple cycles of surface-limited redox replacement (SLRR) were used to grow deposits. Each SLRR involved the underpotential deposition (UPD) of a Cu atomic layer, followed by open circuit replacement via redox exchange with tetrachloropalladate, forming a Pd atomic layer: one E-ALD deposition cycle. That cycle was repeated in order to grow deposits of a desired thickness. 5 cycles of Pd deposition were performed on the Au on glass substrates, resulting in the formation of 2.5 monolayers of Pd. Those Pd films were then modified with varying coverages of Pt, also formed using SLRR. The amount of Pt was controlled by changing the potential for Cu UPD, and by increasing the number of Pt deposition cycles. Hydrogen absorption was studied using coulometry and cyclic voltammetry in 0.1 M H_2SO_4 as a function of Pt coverage. The presence of even a small fraction of a Pt monolayer dramatically increased the rate of hydrogen desorption. However, this did not reduce the films' hydrogen storage capacity. The increase in desorption rate in the presence of Pt was over an order of magnitude.

© The Author(s) 2016. Published by ECS. This is an open access article distributed under the terms of the Creative Commons Attribution Non-Commercial No Derivatives 4.0 License (CC BY-NC-ND, http://creativecommons.org/licenses/by-nc-nd/4.0/), which permits non-commercial reuse, distribution, and reproduction in any medium, provided the original work is not changed in any way and is properly cited. For permission for commercial reuse, please email: oa@electrochem.org. [DOI: 10.1149/2.0051612jes] All rights reserved.

Manuscript submitted April 18, 2016; revised manuscript received July 14, 2016. Published July 28, 2016. *This paper is part of the JES Focus Issue on Electrochemical Deposition as Surface Controlled Phenomenon: Fundamentals and Applications.*

Hydrogen is a valuable fuel for transportation purposes because its energy can be harvested efficiently and it does not generate air pollution in the vicinity of the vehicle. Challenges associated with the compact storage of hydrogen remain an obstacle to its widespread use. Storage in the form of a solid hydride is one way to achieve a high volumetric energy density. While too expensive for automotive hydrogen storage, palladium (Pd) is an often studied material for this purpose due to its high reversibility to charge-discharge cycles, its resistance to oxidation and the low hydrogen gas overpressure required to maintain the hydride state.² Pd forms a surface hydride as well as a non-stoichiometric compound PdH_x in the bulk when hydrogen atoms occupy octahedral sites in the fcc crystal lattice.³ Moreover, the formation of the hydride can occur at room temperature and atmospheric pressure. This ability of Pd to store hydrogen on its surface or in the bulk thus opens up avenues in sensing⁴ and in the storage of hydrogen, as well as a component of fuel cell catalysts.⁵

Electrochemical atomic layer deposition (E-ALD) is the electrochemical version of gas phase ALD. It can be performed at room temperature and used to grow deposits one atomic layer at a time. E-ALD has been used to grow semiconductors and superlattice films.^{6,7} Initially, E-ALD was developed by growing compound semiconductors.^{8–12} With the introduction of surface limited redox replacement (SLRR), ^{13–15} E-ALD became applicable to the growth of metal nanofilms as well. SLRR involves the initial deposition of an atomic layer of a sacrificial metal using underpotential deposition (UPD), ¹⁶ followed by exchange of the UPD layer for a more noble metal via redox replacement with its ionic precursor at open circuit, completing one E-ALD cycle. The cycle can then be repeated as necessary to produce conformal nanofilms of a desired thickness.

Pd electrodeposition has been studied extensively on Au substrates by various groups. For example, Kibler et al.¹⁷ studied the deposition of Pd on Au from chloride containing solutions, while Brankovic et al.¹⁸ were the first to study Pd deposition on Au(111) using SLRR: with Cu UPD as the sacrificial atomic layer. No preferential Pd deposition was observed on steps or defect sites.

One early report of hydrogen absorption in Pd was by Flanagan et al.¹⁹ who studied the progress of hydrogen absorption in palladium wires and noticed that surface processes influenced the absorption of hydrogen. Baldauf and Kolb²⁰ grew ultrathin Pd layers on Au(111) and studied hydrogen sorption in those films. Quaino et al.²¹ used theoretical models to study hydrogen oxidation on submonolayers of Pd on Au(111) and correlated changes in electronic properties and geometric arrangements.

Surface modification has been known to have an effect on the electroactivity of Pd. Czerwinski et al.²² reported the influence of CO on the absorption and desorption of hydrogen. Baldauf and Kolb showed that the presence of crystal violet enhances the hydrogen absorption reaction.²⁰ Bartlett and Marwan report the same effect with crystal violet as well as Pt.²³ Sheridan et al. studied hydrogen sorption into Rh modified Pd films and reported a kinetic enhancement.²⁴

A scheme for the growth of Pd films on Au polycrystalline and single crystal substrates was developed by groups that included authors of this article, and used to study hydrogen sorption.^{25–27} That work demonstrated the ability to achieve flat, uniform, conformal layers over the deposit area. In the present work, the controlled growth of Pd nanofilms on polycrystalline Au substrates, as well as surface modification with Pt using E-ALD, will be described. Those deposits have been used here to extend observations of Bartlett and Marwan.²³ The Pd films maintain the amount of hydrogen stored, even while being covered with Pt and demonstrating higher peak currents for hydrogen desorption. The kinetics of hydrogen desorption from a Pd crystal lattice were studied using coulometry, and the rates for hydrogen desorption have been examined, as have those when the surface has been modified by fractions of a monolayer of Pt. Considering these results, and those from other recent work concerning the enhanced kinetics resulting from Pt surface modification, possible mechanisms are briefly discussed based on the ability to differentiate surface hydride adsorption and bulk hydride absorption in the Pd thin films.

Experimental

Vapor deposited Au on glass slides (100 nm Au on a 5 nm Ti adhesion layer) were used as substrates for all deposits (EMF Corporation).

^bEnergy Nanomaterials Department, Sandia National Laboratories, Livermore, California 94550, USA

 $^{{\}rm *Electrochemical\ Society\ Member.}$

^{**}Electrochemical Society Fellow.

^zE-mail: Stickney@uga.edu

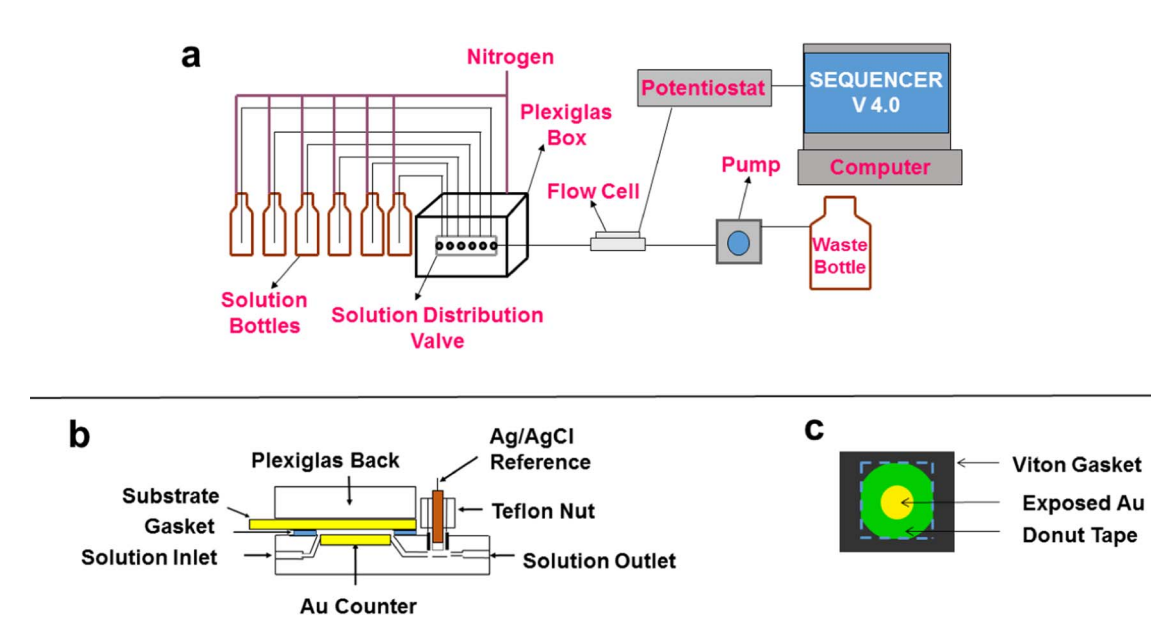


Figure 1. (a) Schematic representation of an E-ALD flow cell system, (b) Lateral view of flow cell and, (c) Top view of Au slide.

Solutions were prepared with 18 M Ω -cm ultrapure water (Milli-Q Advantage A10). The Pd solution was 0.1 mM ultrapure-grade PdCl₂ (Aldrich Chemicals) in 50 mM HCl, in which the tetrachloropal-ladate ion PdCl₄²⁻ is expected to form. The Pt solution was 0.01 mM ultrapure-grade H₂PtCl₆ in 50 mM HClO₄. The Cu solution was 1 mM CuSO₄ and 0.1 M H₂SO₄.

The deposits were grown and studied in an automated electrochemical flow deposition system (Electrochemical ALD L.C., Athens, GA), diagramed in Figure 1. The system consisted of five solution reservoirs, a 5 valve block and a variable speed peristaltic pump. The valves were housed in a Plexiglas box along with the solution reservoirs so they could be purged continuously with N₂, to minimize exposure to O₂. The electrochemical flow cell, downstream from the valves, was also made of Plexiglas and had a volume of around 0.15 mL. A three electrode cell configuration was used, with a Au wire auxiliary electrode embedded in the front cell plate, directly across from the substrate. The reference was a Ag/AgCl electrode (3 M KCl) (Bioanalytical systems) against which all potentials have been reported. E-ALD software "Sequencer-4" was used to control valves, pump and potentials. The Au on glass substrates had an exposed area of 0.71 cm², defined using a piece of Polydonut masking tape (EPSI).

Results and Discussion

Nanofilm formation by E-ALD.—Prior to deposition, the Au substrate was cleaned by cycling in 0.1 M H₂SO₄ from -0.2 V to 1.4 V 3 times at 10 mV/s, followed by 2 cycles in 50 mM HCl from -0.2 V to 0.7 V at 10 mV/s, to produce a more ordered surface.²⁷ Figure 2 is a schematic for the SLRR deposition of Pd, and surface modification of the Pd nanofilms with Pt. The E-ALD cycle for Pd deposition was optimized and studied previously by this group. 24-27 E-ALD has also been used to grow Pt nanofilms on Au. 15,28 The Pt E-ALD cycle used in this study was modified in order to deposit controlled fractions of a monolayer on the Pd nanofilms. Initially an atomic layer of Cu was deposited on Au. This was followed by redox replacement of the Cu by Pd²⁺ ions at open circuit, resulting in an atomic layer of Pd metal. The cycle was repeated to form the Pd thin film. This was followed by depositing another atomic layer of Cu metal and its replacement using Pt⁴⁺ ions, to form a Pd film with its surface modified by Pt.

Figure 3 displays the current-potential-time trace for the Pd cycle, where Cu UPD is followed by Pd replacement. The Cu^{2+} solution was introduced to the cell at 0.15 V and a flow rate of 17 mL/min for 18 s, to

form the sacrificial Cu UPD layer. That was followed by introduction of the Pd^{2+} solution at open circuit, which allowed replacement of the Cu with Pd. Note that in Figure 3 the potential increased during the replacement reaction, finally reaching the programmed stop potential of 390 mV. The stop potential was chosen to prevent Pd oxidation. Reaching the stop potential triggered a blank rinse, during which 0.1 M H_2SO_4 flowed through the cell at the open circuit potential (OCP). The cycle was then repeated a sufficient number of times to produce the desired deposit thickness.

Surface modification with Pt was achieved similarly. The Cu UPD layer was first deposited, followed by introduction of Pt⁴⁺ ions at open circuit. The result was that each Pt⁴⁺ ion received four electrons, by oxidizing the equivalent of two Cu UPD atoms. The resulting Pt coverage on the Pd surface was modified by either adjusting the Cu UPD potential, in order to deposit fractions of a monolayer, or by repeating the cycle to achieve Pt coverages slightly greater than a monolayer. For purposes limited to this paper, we define an amount of charge corresponding to one monolayer ("ML") as 448 μC/cm². This number is based on approximating the surface as a Au(111) surface and two electrons for every Cu atom. The stop potential was maintained at 390 mV to avoid oxidation of the underlying Pd layer. The Pd and Pt coverages were determined using the charge for Cu UPD and assuming 100% exchange efficiency: the coverages reported here are the maximum possible under the conditions used. The relationship between the number of cycles performed and the Pd coverage is shown in Figure 4. In the present study, 5 cycles were grown, each cycle depositing 0.5 ML, resulting in a Pd coverage of 2.5 ML. Some reports suggest that Pd only starts absorbing hydrogen above 2 ML.^{20,29,30} Pd nanofilm coverages were also determined by their oxidative stripping in 50 mM HCl, scanning from 150 mV to 700 mV. The linearity of the graph in Figure 4 is consistent with ALD and layer by layer growth, where doubling the number of cycles doubled the coverage.

Figure 5 displays a cyclic voltammogram (CV) for a 2.5 ML Pd film in 0.1 M H_2SO_4 over the hydrogen sorption region. A negative scan from 150 mV, reversed at -250 mV and ending at 150 mV is demonstrated. This range of potentials corresponds to where H sorption and desorption take place on Pd. The first reduction peak, -8 mV, indicates hydrogen adsorption, or some surface hydride formation (UPD H) on Pd. The second broad feature, at -200 mV, indicates hydrogen absorption into bulk Pd, and is followed by absorption convoluted with H_2 evolution near -250 mV. Absorption into the bulk leads to the formation of the β -hydride (PdH_x). After reversal of

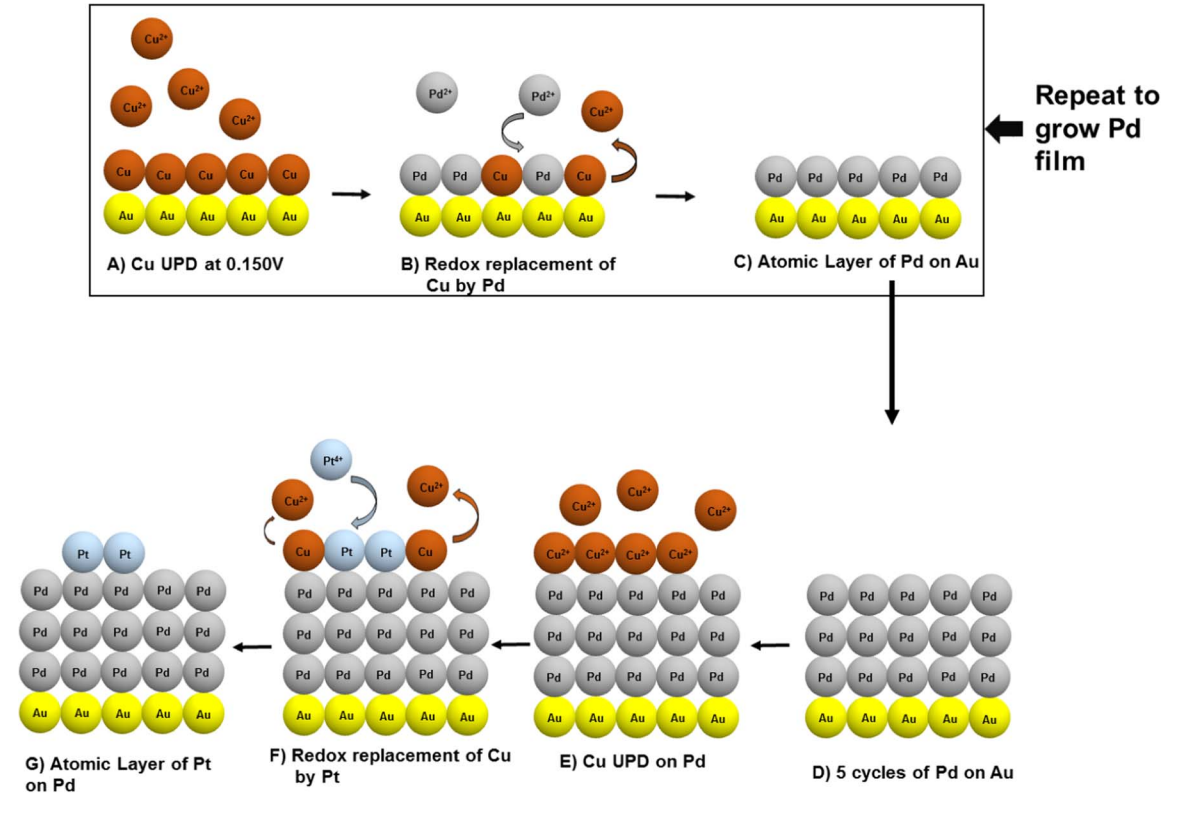


Figure 2. Schematic of E-ALD SLRR cycles for Pd and Pt.

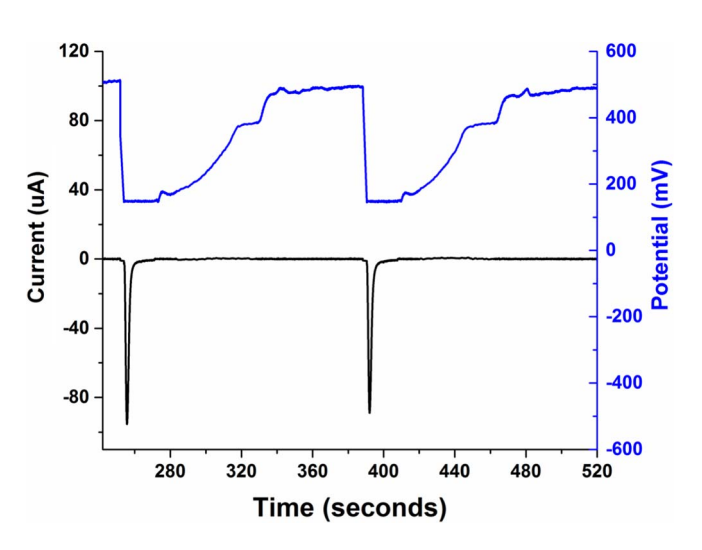
the potential scan at -250 mV, hydrogen desorption began, peaking near -200 mV. Desorption of the adsorbed layer of hydrogen atoms (H UPD) is peaked at 0 mV. The adsorption and absorption characteristically occur at different potentials on thin films. In similar CVs using thicker films or bulk Pd, surface hydride peaks are not normally observed because of the large currents for H absorption and its subsequent desorption, relative to H UPD.³²

Based on the CV in Figure 5, a potential sequence was designed to first saturate the Pd film with hydrogen at negative potential, followed by stepping the potential to 0 mV and using coulometry to determine how much hydrogen desorbed. That is, the films were initially equilibrated in 0.1 M H₂SO₄ at 150 mV for 10 s (point X) then stepped to -250 mV for 5 min (point Y) to saturate the Pd film with hydrogen. To determine the amount of absorbed hydrogen, the potential was

stepped from -250 mV to 0 mV (point Z) for 10 s, to strip absorbed hydrogen.

Figure 6 is an example of chronoamperometry for hydrogen oxidation on a 2.5 ML Pd thin film. Integration of the current peak was used to determine the moles of hydrogen in the Pd film.

The moles of Pd in the film were determined by using the sum of the coulometry for Cu UPD from each Pd SLRR cycle used to grow the film. Saturation H/Pd molar ratios have been reported between 0.6 to $0.8.^{22,24,27,31,33-35}$ Values near 0.7 for the H/Pd ratio were obtained for the present Pd films. Charges for hydrogen oxidation were used rather than hydrogen absorption in order to avoid issues with distinguishing charge due to H_2 evolution from charge due to absorption.



R² = 0.9979

Figure 3. Current-Potential-Time trace illustrating the Pd E-ALD cycles.

Figure 4. Plot of Pd coverage vs. the number of cycles performed.

3.0

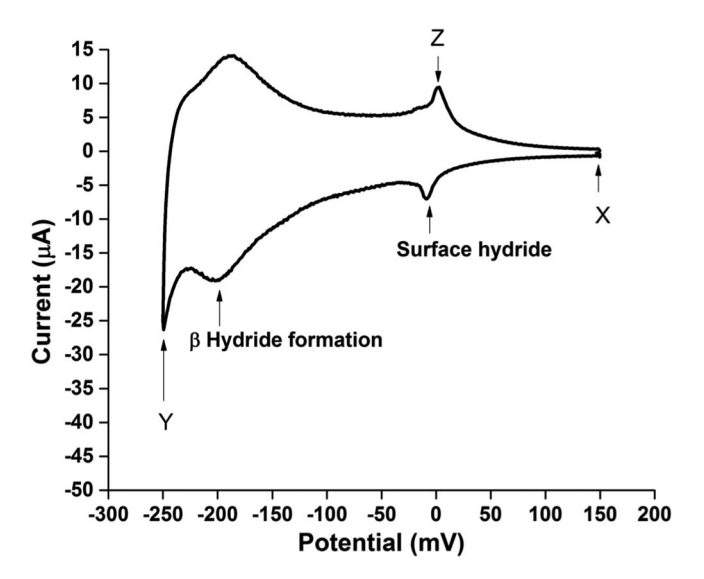


Figure 5. CV of 2.5 ML Pd nanofilm in 0.1 M H₂SO₄, performed at 10 mV/s. Potentials used for charging and discharging the film with hydrogen, indicated by X, Y and Z, are discussed in text.

Figure 7 displays the H/Pd ratio as a function of the amount of Pt modifying the Pd surface. No significant effect was observed on the H/Pd ratio as a function of the Pt coverage, in contrast to values reported in the literature for Pd-Pt alloys. For alloys, the capacity (H/Pd ratio) decreased rapidly with increasing amounts of Pt, approaching complete loss of its ability to store H for alloys with a Pt mole fraction above 19%. 36-40

Kinetics of hydrogen desorption.—Figure 8 compares the hydrogen oxidation currents for unmodified and modified Pd films. It indicates that the presence of even 0.01 ML of Pt on the Pd surface causes a dramatic increase in the hydrogen oxidation current. In addition, the current decays to zero much faster with Pt present, indicating that hydrogen desorbs much faster when Pt is on the surface.

Curve fits.—A biexponential function, including an offset current (I_o) , was shown to provide a good fit to the decay of the chronoamperometric curves shown in Figure 8. Those results were used to investigate changes in the mechanism of hydrogen desorption with and without

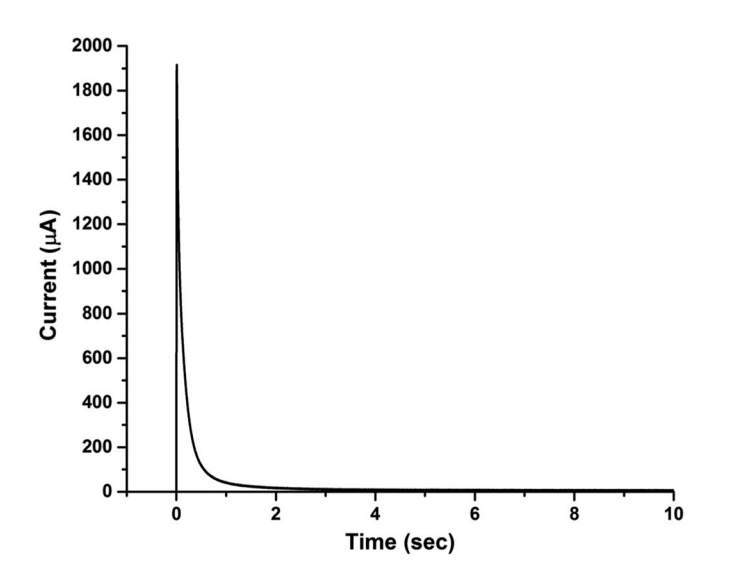


Figure 6. Hydrogen oxidation chronoamperometry for a 2.5 ML thin film saturated with hydrogen, on stepping from -250 mV to 0 mV.

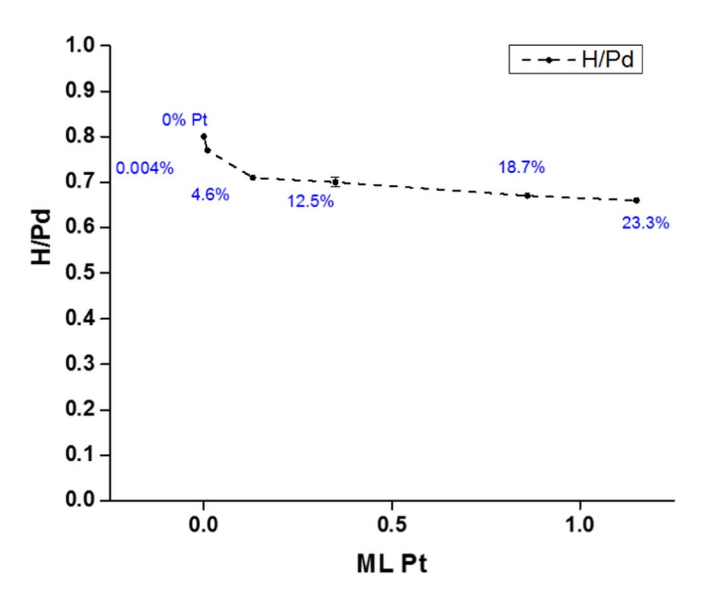


Figure 7. H/Pd ratio with increasing Pt coverage with Pt coverage shown as % within the figure.

Pt present. The offset current might be attributable to background processes such as oxidation of aqueous H_2 . A simple interpretation of the biexponential function is that there are two independent processes, such as absorption and adsorption, each with capacities, C_1 and C_2 (mol H/mol Pd), within the film. Each have a different first-order rate constant, the reciprocals of which would be the time constants t_1 and t_2 . This can be expressed as:

$$I = I_0 + \frac{FAC_1d}{Mt_1}e^{-t/t_1} + \frac{FAC_2d}{Mt_2}e^{-t/t_2}$$
 [1]

where F is the Faraday constant (coulombs/mol), A is the electrode area (cm²), d is the film thickness (cm), and M is the molar volume of palladium (cm³/mol). The capacities C_1 and C_2 can be related to the ratio of the charge for hydrogen absorption and half the charge for Pd stripping. This number is also the molar H/Pd ratio.

A plot of the time constants versus the Pt coverage (Figure 9) shows that even a small amount of Pt on the surface results in an increase in the kinetics of the hydrogen oxidation reaction. For the coverages studied, the time constants dropped with increasing Pt coverage, plateauing near a ML. The presence of two time constants may indicate parallel processes for hydrogen desorption from Pd. It is

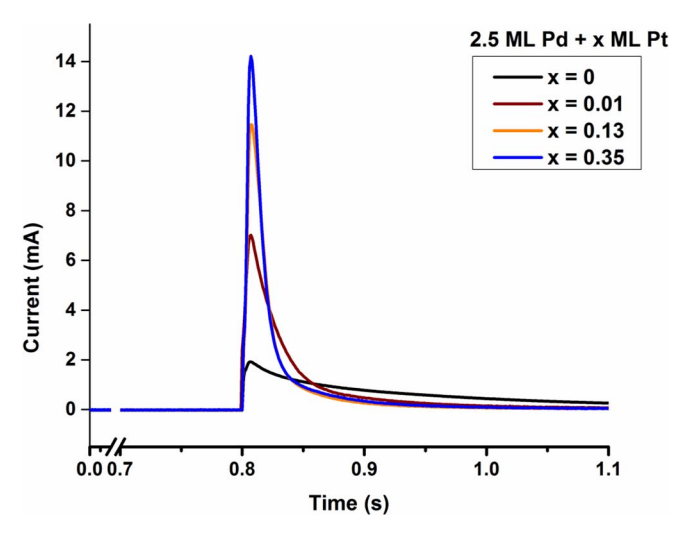


Figure 8. Comparison of H oxidation currents for Pd and Pt modified Pd films

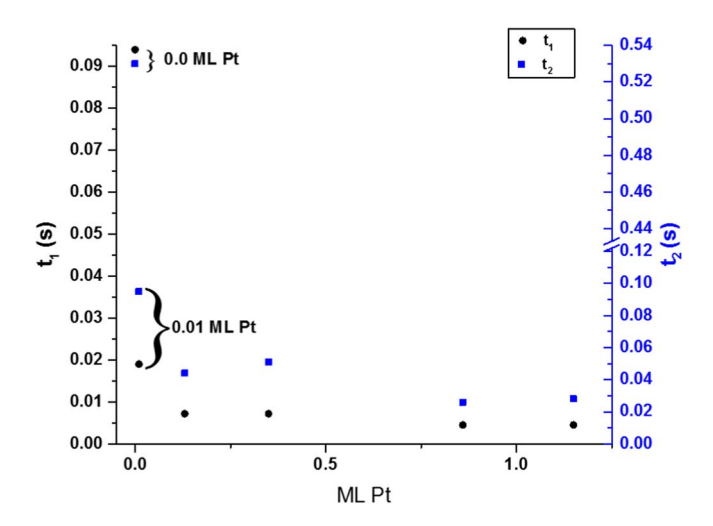


Figure 9. Decay constants for desorption of hydrogen from bare 2.5 ML Pd and Pt modified Pd thin films.

possible that the hydrogen present within the crystal structure is desorbed quickly (characterized by t_1) and the second time constant (t_2) could be measuring desorption of H at or near surfaces or grain boundaries, or from the dilute α phase. However, the time constants show a similar trend in their decrease with increasing Pt present on the surface, indicating faster desorption for each process.

Mechanism.—Numerous theories have been presented regarding the mechanism of hydrogen absorption into Pd. Jerkiewicz et al. 41 describe an indirect mechanism for hydrogen absorption into Pd. According to that mechanism, the hydrogen is first adsorbed on the electrode surface (UPD H). The surface hydrogen moves into empty subsurface sites, followed by diffusion into the bulk to form a non-stoichiometric compound (PdH_x). Bartlett et al. 23 suggest a direct absorption of hydrogen into Pd that occurs in a single step:

$$H_3O^+ + e^- \rightarrow H_{abs} + H_2O$$
 [2]

This is based on their observation that UPD H peaks are greatly diminished in their voltammograms in the presence of surface Pt. They suggest that the surface hydride acts as a spatial obstacle that blocks direct absorption. The extreme tendency for Pt to adsorb trace contaminants must however be kept in mind.

The work presented here was undertaken in response to the theoretical work of Greeley and Mavrikakis, ⁴² which supports the indirect mechanism. In that scenario, the surface hydride is destabilized in the presence of Pt, shifted to a potential near that for bulk absorption, or a distribution of potentials between the UPD peak and absorption peak. The destabilized surface hydride has a lower activation barrier to enter bulk states, leading to faster absorption and desorption rates

Figure 10 compares CVs for a 2.5 ML Pd film and a 2.5 ML Pd film modified with 0.1 ML Pt, in 0.1 M $\rm H_2SO_4$. A clear reduction of the surface hydride peak at -8 mV occurs when Pt is present. A prior report of the E-ALD of a Pt multilayer film on $\rm Au^{28}$ using similar conditions showed hydride peaks at +50 mV and -100 mV, though only after the surfaces were cleaned via oxidative cycles. This suggests that the surface hydrides on the Pd surface are modified into a distribution of stabilities in the presence of Pt, some of which are more or less stable than for pure Pd. Contaminants adsorbed to the Pt may have some influence on surface hydride formation, but based on our observations, any such contaminants that are present do not inhibit transport of hydrogen between the electrode and solution.

It is not proposed here that the surface hydride is so destabilized in the presence of Pt that it is not present at all, as would be necessary to spatially unblock the direct pathway, as described by Bartlett

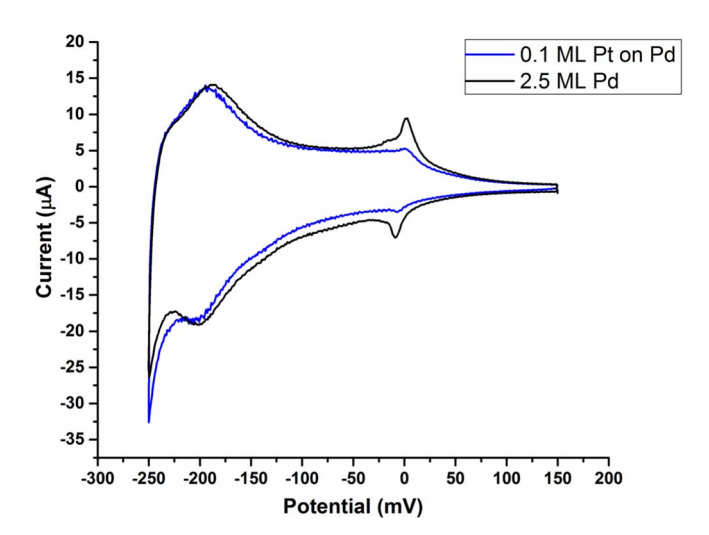


Figure 10. CVs of 2.5 ML Pd nanofilm in 0.1 M H_2SO_4 (black line) and 2.5 ML Pd film modified with 0.1 ML Pt on the surface (blue line), performed at 10 mV/s. Note the reduction in surface hydride when Pt is present on the surface.

et al.²³ If that were the case, it would not be possible to grow multiple cycles of Pt using the surface hydride as the sacrificial layer, as was shown by Vasiljevic et al.⁴³ and this group. By that argument, the indirect mechanism is more consistent with reported observations. Another consideration described by Łukaszewski et al.⁴⁴ is that the transition from the solid solution (α phase) to the formation of the non-stoichiometric compound (β phase) involves rearrangement of Pd atoms, and not just hydrogen atoms. If the rearrangement of Pd atoms is slow, this could be the rate-limiting step, instead of transport of hydrogen between surface and bulk. The fact that various groups, in addition to this one, have observed strong effects from surface modification suggests that the Pd atom rearrangement is not the rate-limiting step, at least in the case of nanometer-scale films or porous structures.

Conclusions

When the surfaces of Pd nanofilms were modified with Pt, peak hydrogen oxidation currents increased, even with submonolayer amounts of Pt, indicating a catalytic effect on the reaction. Fits to a simple kinetic model showed enhancement of the oxidative hydrogen desorption rate for films coated with Pt by over an order of magnitude, though the enhancement was not greatly sensitive to the amount of Pt present for coverages near a ML. The H/Pd ratio did not change significantly as a function of the amount of deposited Pt, suggesting it remained as a surface layer, and did not form an alloy.

When considered in the context of other recent work, the results described here support a mechanism in which hydrogen absorption and desorption are mediated by a surface hydride, and each process can be limited by desorption of the surface hydride into the aqueous or bulk solid phase. The presence of Pt on the surface destabilizes some of the surface hydride sites, accelerating hydrogen transport between surface and bulk. Proper understanding of this mechanism is likely to be important in the development of hydrogen storage and separation devices that use palladium, and perhaps other materials where surface species are important.

Acknowledgments

We acknowledge the support of the National Science Foundation, Division of Materials Research no. 1410109 and the Laboratory-Directed Research and Development program at Sandia National Laboratories, a multiprogram laboratory managed and operated by Sandia Corporation, a wholly owned subsidiary of Lockheed Martin Corporation, for the U.S. Department of Energy's National Nuclear Security Administration under contract DE-AC04-94AL85000.

References

- G. W. Crabtree, M. S. Dresselhaus, and M. V. Buchanan, *Physics Today*, 57(12), 39 (2004).
- P. N. Bartlett, B. Gollas, S. Guerin, and J. Marwan, *Phys. Chem. Chem. Phys.*, 4(15), 3835 (2002).
- T. B. Flanagan and W. A. Oates, Annual Review of Materials Science, 21(1), 269 (1991).
- F. Favier, E. C. Walter, M. P. Zach, T. Benter, and R. M. Penner, *Science*, 293(5538), 2227 (2001).
- 5. E. Antolini, Energy & Environmental Science, 2(9), 915 (2009).
- 6. J. L. Stickney, Advances in Electrochemical Science and Engineering, 7, 1 (2002).
- M. Cavallini, M. Facchini, C. Albonetti, F. Biscarini, M. Innocenti, F. Loglio, E. Salvietti, G. Pezzatini, and M. L. Foresti, *The Journal of Physical Chemistry* C, 111(3), 1061 (2007).
- 8. B. W. Gregory and J. L. Stickney, *Journal of Electroanalytical Chemistry and Inter-facial Electrochemistry*, **300**(1–2), 543 (1991).
- D. O. Banga, R. Vaidyanathan, L. Xuehai, J. L. Stickney, S. Cox, and U. Happeck, *Electrochim. Acta*, 53(23), 6988 (2008).
- T. L. Wade, L. C. Ward, C. B. Maddox, U. Happek, and J. L. Stickney, *Electrochemical and Solid-State Letters*, 2(12), 616 (1999).
- M. L. Foresti, G. Pezzatini, M. Cavallini, G. Aloisi, M. Innocenti, and R. Guidelli, J. Phys. Chem. B, 102(38), 7413 (1998).
- 12. B. E. Boone and C. Shannon, Journal of Physical Chemistry, 100(22), 9480 (1996).
- 13. M. F. Mrozek, Y. Xie, and M. J. Weaver, Anal. Chem., 73(24), 5953 (2001).
- R. Vasilic and N. Dimitrov, *Electrochemical and Solid-State Letters*, 8(11), C173 (2005).
- Y.-G. Kim, J. Y. Kim, D. Vairavapandian, and J. L. Stickney, *The Journal of Physical Chemistry B*, 110(36), 17998 (2006).
- 16. A. A. Gewirth and B. K. Niece, Chem. Rev., 97, 1129 (1997).
- L. A. Kibler, M. Kleinert, R. Randler, and D. M. Kolb, *Surface Science*, 443(1–2), 19 (1999).
- S. R. Brankovic, J. X. Wang, and R. R. Adžić, Surface Science, 474(1-3), L173 (2001).
 T. B. Flancon and F. A. Lewis, Transactions of the Eurodean Society, 55(0), 1400.
- T. B. Flanagan and F. A. Lewis, Transactions of the Faraday Society, 55(0), 1400 (1959).
- 20. M. Baldauf and D. M. Kolb, *Electrochim. Acta*, 38(15), 2145 (1993).
- P. Quaino, E. Santos, H. Wolfschmidt, M. Montero, and U. Stimming, *Catalysis Today*, 177(1), 55 (2011).
- A. Czerwiński, S. Zamponi, and R. Marassi, Journal of Electroanalytical Chemistry and Interfacial Electrochemistry, 304(1-2), 233 (1991).

- 23. P. N. Bartlett and J. Marwan, *Phys. Chem. Chem. Phys.*, 6(11), 2895 (2004).
- L. B. Sheridan, V. M. Yates, D. M. Benson, J. L. Stickney, and D. B. Robinson, *Electrochim. Acta*, 128(0), 400 (2014).
- L. B. Sheridan, J. Czerwiniski, N. Jayaraju, D. K. Gebregziabiher, J. L. Stickney, D. B. Robinson, and M. P. Soriaga, *Electrocatalysis*, 3(2), 96 (2012).
- L. B. Sheridan, D. K. Gebregziabiher, J. L. Stickney, and D. B. Robinson, *Langmuir*, 29(5), 1592 (2013).
- 27. L. B. Sheridan, Y. G. Kim, B. R. Perdue, K. Jagannathan, J. L. Stickney, and
- D. B. Robinson, *J. Phys. Chem. C*, **117**(30), 15728 (2013).
 N. Jayaraju, D. Vairavapandian, Y. G. Kim, D. Banga, and J. L. Stickney, *J. Electrochem. Soc.*, **159**(10), D616 (2012).
- B. Álvarez, A. Berná, A. Rodes, and J. M. Feliu, *Surface Science*, 573(1), 32 (2004).
- J. Tang, M. Petri, L. A. Kibler, and D. M. Kolb, *Electrochim. Acta*, 51(1), 125 (2005).
- P. Bartlett, B. Gollas, S. Guerin, and J. Marwan, *Phys. Chem. Chem. Phys.*, 4(15), 3835 (2002).
- A. Czerwiński, I. Kiersztyn, M. Grdeń, and J. Czapla, *Journal of Electroanalytical Chemistry*, 471(2), 190 (1999).
- 33. H. A. Rafizadeh, *Physical Review B*, 23(4), 1628 (1981).
- C. Gabrielli, P. P. Grand, A. Lasia, and H. Perrot, *J. Electrochem. Soc.*, 151(11), A1937 (2004).
- J. L. Stickney, L. Sheridan, and D. Robinson, Abstr. Pap. Am. Chem. Soc., 244, (2012).
- M. Grden, A. Piascik, Z. Koczorowski, and A. Czerwinski, *Journal of Electroanalytical Chemistry*, 532(1-2), 35 (2002).
- M. Łukaszewski, M. Grdeń, and A. Czerwiński, Journal of New Materials for Electrochemical Systems, 9, 409 (2006).
- M. Lukaszewski, K. Hubkowska, and A. Czerwinski, *Phys. Chem. Chem. Phys.*, 12(43), 14567 (2010).
- M. Łukaszewski, A. Żurowski, M. Grdeń, and A. Czerwiński, *Electrochemistry Communications*, 9(4), 671 (2007).
- I. Moysan, V. Paul-Boncour, S. Thiébaut, E. Sciora, J. M. Fournier, R. Cortes, S. Bourgeois, and A. Percheron-Guégan, *Journal of Alloys and Compounds*, 322(1–2), 14 (2001).
- 41. G. Jerkiewicz and A. Zolfaghari, J. Electrochem. Soc., 143(4), 1240 (1996).
- J. Greeley and M. Mavrikakis, The Journal of Physical Chemistry B, 109(8), 3460 (2005).
- J. Nutariya, M. Fayette, N. Dimitrov, and N. Vasiljevic, *Electrochim. Acta*, 112(0), 813 (2013).
- M. Lukaszewski, K. Klimek, A. Zurowski, T. Kedra, and A. Czerwinski, Solid State Ion., 190(1), 18 (2011).